ATLAS Transition Radiation Tracker Test Beam Results

T. Akesson [a], E. Arik [b], K. Baker [c], S. Baron [d], D. Benjamin [e], H. Bertelsen [f], V. Bondarenko [g], V. Bytchkov [h], J. Callahan [i], M. Capeans [d], L. Cardiel-Sas [d], A. Catinaccio [d], S.A. Cetin [b], P. Cwetanski [d], M. Dam [f], H. Danielsson [d], F. Dittus [d], B. Dolgoshein [g], N. Dressnandt [j], C. Driouichi [a], W.L. Ebenstein [e], P. Eerola [a], P. Farthouat [d], O. Fedin [k], D. Froidevaux [d], P. Gagnon [i], Y. Grichkevitch [ℓ], N. Grigalashvili [h], Z. Hajduk [m], P. Hansen [f], F. Kayumov [n,i], P.T. Keener [j], G. Kekelidze [h], A. Khristatchev [k], S. Konovalov [n], L. Koudine [k], S. Kovalenko [k], T. Kowalski [o], V.A. Kramarenko [ℓ], K. Kruger [d], A. Laritchev [ℓ], P. Lichard [d], F. Luehring [i], B. Lundberg [a], V. Maleev [k], I. Markina [g], K. McFarlane [c], V. Mialkovski [h], V.A. Mitsou [d], B. Mindur [o], S. Morozov [g], A. Munar [j], S. Muraviev [n], A. Nadtochy [k], F.M. Newcomer [j], H. Ogren [i], S.H. Oh [e], S. Oleshko [k], J. Olszowska [m], S. Passmore [d], S. Patritchev [k], V. Peshekhonov [h], R. Petti [d], M. Price [d], C. Rembser [d], O. Rohne [j], A. Romaniouk [d,g], D.R. Rust [i], Yu. Ryabov [k], V. Schegelsky [k], D. Seliverstov [k], T. Shin [c], A. Shmeleva [n], S. Smirnov [g], V. Sosnovtsev [g], V. Soutchkov [g], E. Spiridenkov [k], V. Tikhomirov [n,*], R. Van Berg [j], V. Vassilakopoulos [c], L. Vassilieva [n], C. Wang [e], H.H. Williams [j], A. Zalite [k]

[a] *Fysiska Institutionen, Lunds Universitet, Lund, Sweden*
[b] *Department of Physics, Bogazici University, Istanbul, Turkey*
[c] *Hampton University, Hampton, Virginia, USA*
[d] *European Laboratory for Particle Physics (CERN), Geneva, Switzerland*
[e] *Physics Department, Duke University, Durham, North Carolina, USA*
[f] *Niels Bohr Institute, University of Copenhagen, Copenhagen, Denmark*
[g] *Moscow Engineering and Physics Institute, Moscow, Russia*
[h] *Joint Institute of Nuclear Research, Dubna, Russia*
[i] *Department of Physics, Indiana University, Bloomington, Indiana, USA*
[j] *Department of Physics and Astronomy, University of Pennsylvania, Philadelphia, Pennsylvania, USA*
[k] *Petersburg Nuclear Physics Institute, Gatchina, St. Petersburg, Russia*
[ℓ] *Moscow State University, Institute of Nuclear Physics, Moscow, Russia*
[m] *Henryk Niewodniczanski Institute of Nuclear Physics, Cracow, Poland*
[n] *P.N. Lebedev Institute of Physics, Moscow, Russia*
[o] *Faculty of Physics and Nuclear Techniques of the Academy of Mining and Metallurgy, Cracow, Poland*

Abstract

Several prototypes of the Transition Radiation Tracker for the ATLAS experiment at the LHC have been built and tested at the CERN SPS accelerator. Results from detailed studies of the straw-tube hit registration efficiency and drift-time measurements and of the pion and electron spectra without and with radiators are presented.

Key words: ATLAS, TRT, Test-beam, Transition radiation, Drift-time measurement, Energy loss spectra
PACS: 29.40.Gx

1. Experimental set-up

The Transition Radiation Tracker (TRT) [1] is one of the components of the ATLAS Inner Detector [2]. It combines electron identification capability with charged-particle track reconstruction. This is achieved by interleaving layers of xenon-filled drift tubes of small diameter (straws) with radiators. In order to test the physics performance of the proposed detector, several small-scale TRT prototypes were built and tested in the H8 beam line at the CERN SPS accelerator over the past twelve years. Results from these TRT test-beam analyses have been reported in [3–6]. Recent results on the TRT performance at high counting rates, obtained with high-rate prototype, can be found in [7]. The most important results obtained in the years 2000-2002 with small radiator/straw prototypes and with an end-cap TRT sector prototype are presented here.

The TRT performance was evaluated using electron, pion and muon beams with energies varying from 5 to 300 GeV. The typical layout of the test-beam set-up is shown in Fig. 1. Three precise silicon microstrip detectors (Si1, Si2, Si3) with an intrinsic resolution of 10 μm and two gaseous beam chambers (BC1, BC2) formed a beam telescope. Two Cherenkov counters (Ch1, Ch2) and a preshower detector together with a small lead-glass electromagnetic calorimeter were used for beam-particle identification with a π/e rejection factor of 10^{-5}.

Straws, the detector elements of the TRT, are tubes of 4 mm diameter made from a conductive

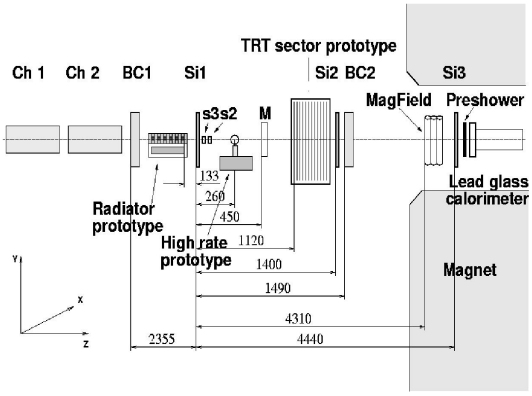

Fig. 1. Experimental set-up in the 2002 test-beam run. All distances are in mm. The drawing is not to scale.

polyimide (Kapton) film. The anode wires, made from gold-plated tungsten, have a diameter of 30 μm. For all measurements made before 2002, the straws were operated with a gas mixture consisting of 70%Xe+20%CF_4+10%CO_2. More recently, the TRT prototypes were operated with a new gas mixture, consisting of 70%Xe+27%CO_2+3%O_2, which was chosen to solve etching problems observed with the glass wire-joint in the barrel TRT straws with the original gas mixture (see Ref. [7] for details). The nominal gas gain was $2.5{\cdot}10^4$.

2. Sector prototype

The sector prototype represents 1/32 (11.25^o in azimuth) of one TRT end-cap 16-plane wheel. The space between the 16 layers of radially oriented straws is filled with radiator made from polypropylene foils. This prototype was used for studies of the front-end and back-end electronics and of the

* Corresponding author. Tel: +7-095-132-60-32, fax: +7-095-135-78-80.
E-mail address: Vladimir.Tikhomirov@cern.ch

single-straw drift-time measurement performance, in terms of accuracy, efficiency, noise and overall uniformity of the results across the whole detector.

The sector prototype was equipped with the readout electronics designed for operation of the TRT at the LHC: the ASDBLR analogue chip and the DTMROC digital chip [4,8,9]. The ASDBLR chip contains an amplifier, a shaper for the ion-tail cancellation, a baseline restorer and two discriminators with adjustable thresholds. The low-level threshold is then fed into the DTMROC chip, where it is digitised with a 3.125 ns binning for drift-time measurements. The high-level threshold is used to identify the absorbed transition-radiation (TR) photons. Drift-time information from the straws is stored in three sequential time slices of 25 ns each, corresponding to three consecutive LHC bunch-crossings.

The reference position of the beam-particle track was reconstructed using information from the Si-microstrip telescope. Fig. 2 shows the correlation between the measured drift-time in one straw and the distance between the anode wire and the extrapolated position of the beam-particle track. The distance-to-time relationship for the straw was obtained by fitting each of the left and right branches with a third-degree polynomial. Once the parameters of the above fit are known, the drift-time measurement for each straw can be converted into the distance from the straw anode, and the residual with respect to the position of the extrapolated track can be extracted. The drift-time accuracy σ was then derived from a Gaussian fit to the residual distribution.

Two different efficiencies were then defined for each straw. The first one, called hit-registration efficiency, was defined as the probability for obtaining a low-level threshold hit when a beam particle crosses the straw. The second one, called drift-time measurement efficiency, was defined as the probability for finding the drift-time measurement within a $\pm 2.5 \cdot \sigma$ window from the beam-particle track.

Fig. 3 shows the straw drift-time accuracy and the straw hit-registration and drift-time efficiencies as a function of the low-level threshold for the new gas mixture and for the final front-end electronics chips. For a threshold of 250 eV, the overall drift-time accuracy is 132 μm with independent contributions of about 110 μm from the intrinsic straw and analogue front-end chip performance and of about 50 microns from the 3.125 ns size of the time bins in the digital front-end chip. This performance can be achieved at low counting rates with an efficiency of 87% and the corresponding overall straw hit-registration efficiency is close to 96%. The results obtained at high counting rates are presented in [7].

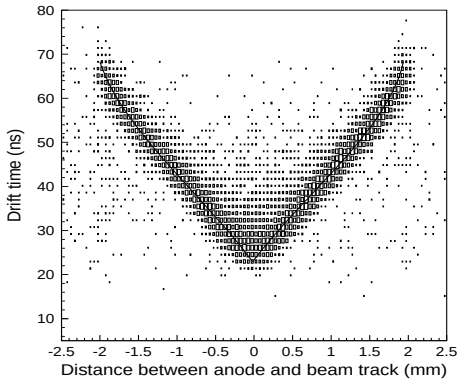

Fig. 2. A typical measured relationship between drift time and distance from extrapolated beam-particle track to a straw anode wire (histogram). The curves represent third-degree polynomial fits to each branch of the distribution.

The straw noise probability was also measured and found to decrease rapidly as the threshold increases, from 11% at 200 eV to 1.1% at 400 eV integrated over three time slices of 25 ns. Taking this into account, a reasonable choice of low-level threshold for operation of the TRT at the LHC was found to be 250 eV, corresponding to a single-straw noise probability of 4.6%.

A special study of possible channel-to-channel cross-talk effects in the sector prototype was performed. Noise arising from cross-talk is potentially more dangerous than the random thermal noise discussed above. This is because cross-talk noise is correlated with real hits in space and time, and may thus create difficulties for the pattern recognition. The measurements have shown that the main cross-talk component is observed between straws belonging to a group of eight channels corresponding to the same ASDBLR chip. The cross-talk probability grows with the largest signal am-

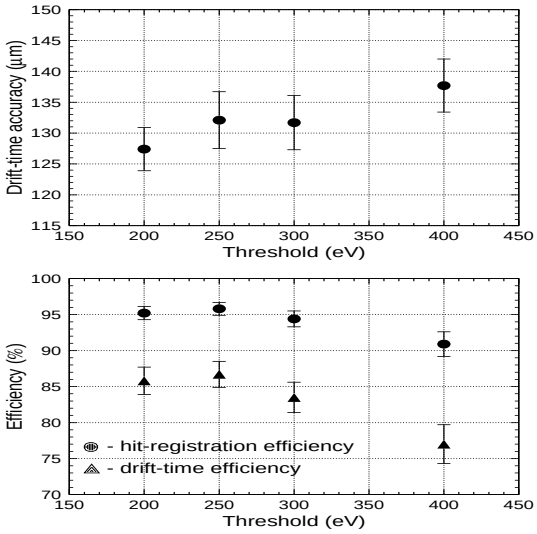

Fig. 3. Drift-time accuracy (top) and hit-registration and drift-time efficiencies (bottom) for a single straw as a function of the low-level threshold on the analogue chip. The error bars represent the variations observed from straw to straw in the sector prototype.

plitude observed in the chip. This effect is therefore more pronounced for electrons, which produce a large number of high-amplitude signals on the track due to the absorbed TR photons. This cross-talk probability drops however rapidly as the low-level threshold increases.

For a threshold of 250 eV, an average of three extra hits from cross-talk are expected for an electron track reconstructed in the ATLAS TRT detector. For charged pions, this average is expected to be five times smaller. Since the total number of low-threshold hits per reconstructed track is expected to be close to 35 on average, the impact of this effect on pattern recognition will be very small.

3. Radiator prototype

The radiator prototype consisted of ten straw layers interleaved with removable radiator blocks. Contrary to the sector prototype, where only two levels of discrimination were available, this prototype had a 10-bit ADC connected to each of the straw outputs to measure accurate $\mathrm{d}E/\mathrm{d}x$ and transition radiation spectra in the straws. With the radiator blocks removed from the prototype, pure $\mathrm{d}E/\mathrm{d}x$ measurements were obtained. Different types of radiators were then introduced to measure their transition-radiation yield.

The position of the beam-particle track in the radiator prototype was found using the Si-microstrip telescope. Fig. 4 presents the measured spectra for different particle types and energies. A clear enhancement of the energy deposition due to the absorbed TR photons can be seen in the case of electrons with radiator.

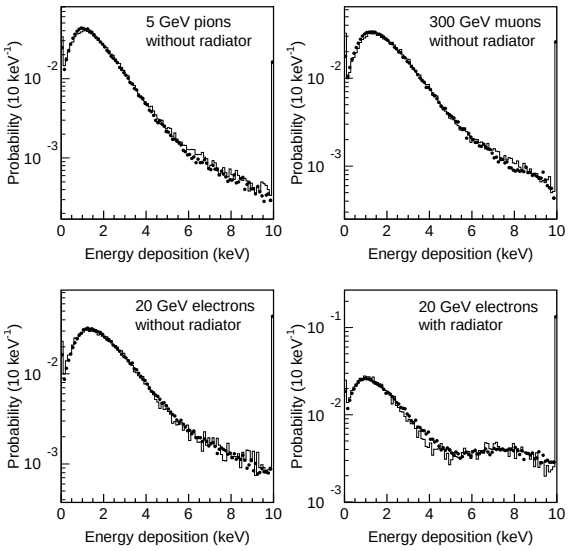

Fig. 4. Differential spectra of energy depositions in a single straw for different particle types and energies without and with radiator. The histograms represent the measured spectra and the dots represent the corresponding Monte-Carlo simulation. All energy depositions above 10 keV are collected in the last bin.

A dedicated Monte-Carlo program [10] has been developed to simulate accurately the $\mathrm{d}E/\mathrm{d}x$ and TR energy deposition in a TRT straw. Fig. 4 shows the excellent agreement between the data and the Monte-Carlo simulation in all cases. A precise quantitative agreement between the test-beam data and Monte-Carlo simulation is crucial in order to predict correctly the electron/pion separation for the TRT detector in ATLAS. One example of small effects, which have to be taken into account, is shown in Fig. 5. This shows that, for energy depositions above 8 keV, the agreement

between test-beam data and Monte-Carlo simulations for electrons is significantly improved when the production of transition radiation in the straw walls is included in the simulation.

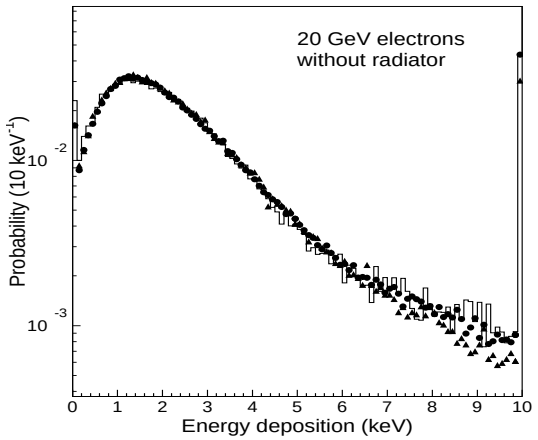

Fig. 5. Differential spectra of energy deposition in a single straw for 20 GeV test-beam electrons without radiator. The histogram represents the measured spectrum. The triangles represent the Monte-Carlo simulation without accounting for transition radiation produced in the straw walls. The dots represent the Monte-Carlo simulation with proper accounting of TR produced in the straw walls. All energy depositions above 10 keV are collected in the last bin.

4. Conclusions

The construction of the mechanical modules and front-end electronics boards for the ATLAS Transition Radiation Tracker (TRT) is now well under way. The validation of the design of many of the components and of the new gas mixture, 70%Xe+27%CO_2+3%O_2, has been partially done using small-scale set-ups in beam tests.

Measurements using components of the final front-end electronics have shown that, for a low-level discriminator threshold of 250 eV, a hit-registration efficiency of 96%, a drift-time accuracy of 132 μm and a drift-time efficiency of 87% can be achieved at low counting rates. Measured differential spectra from dE/dx and transition radiation are in good agreement with Monte-Carlo simulations. As discussed in detail in [7], adequate performance has also been demonstrated up to straw counting rates of 20 MHz, corresponding to those expected for the most exposed straws during operation at the design LHC luminosity.

5. Acknowledgements

We are very grateful to P.Nevski for his contributions to the test-beam and Monte Carlo software. The research described in this publication was partly supported by the following funding agencies: the European Union (DGXII), the International Science Foundation (grant NM5J000), the Swedish Research Council, the State Committee for Scientific Research, Poland (grants 620/E-77/SPUB-M/CERN/P-03/DZ295/2000-2002 and 112/E-356/SPB/CERN/PO3/DZ108/2003-2005) the International Science and Technology Centre (ISTC projects 441 and 1800P), the Civil Research and Development Foundation (grant REC-011) and grants from the U. S. Department of Energy and National Science Foundation.

References

[1] ATLAS Inner Detector Technical Design Report, CERN/LHCC/97-16, CERN/LHCC/97-17, 1997.

[2] ATLAS Technical Proposal, CERN/LHCC/94-43, 1994.

[3] T. Akesson, et al., Nucl. Instrum. and Meth. A 412 (1998) 200.

[4] T. Akesson, et al., Nucl. Instrum. and Meth. A 449 (2000) 446.

[5] T. Akesson, et al., Nucl. Instrum. and Meth. A 474 (2001) 172.

[6] T. Akesson, et al., Nucl. Instrum. and Meth. A 485 (2002) 298.

[7] T. Akesson, et al., Operation of the ATLAS Transition Radiation Tracker under very high irradiation at the CERN LHC. Nucl. Instrum. and Meth. A, this issue.

[8] C. Alexander, et al., IEEE Trans. Nucl. Sci. 48 (2001) 514.

[9] T. Akesson, et al., Status of design and construction of the ATLAS TRT. Nucl. Instrum. and Meth. A, this issue.

[10] P. Nevski, Advances in the simulation of transition radiation detectors. Nucl. Instrum. and Meth. A, this issue.